Comparative Analysis of Process Parameters in Wear Properties of Coated and Uncoated Tool Inserts during Machining of Hastelloy C-276

Bandaru Kiran
B.Tech, School of Mechanical Engineering (SMEC)
Vellore Institute of Technology (VIT)
Vellore, Tamil Nadu
India

Dega Nagaraju
Professor
Department of Manufactring Engineering
School of Mechanical Engineering (SMEC)
Vellore Institute of Technology (VIT)
Vellore, Tamil Nadu
India

Machining is the most significant process for any manufacturing company to improve the quality of the finished component. The objective of this article is to analyse the process performance of Hastelloy C-276 using PVD (Physical Vapour Deposition) coated, uncoated and alumina-based ceramic tool inserts of high grade quality. Turning process was performed on NC (Numerical Control) machine by varying RPM, feed rate and depth of cut based on the Taguchi L9 orthogonal array approach. In this study, crank wear, flank wear, nose wear, SR (Surface Roughness), MRR (Material Removal Rate), tool temperature and feed force are examined during machining of hardened material and simultaneously static structural analysis of the tool insert along with the tool holder was performed using ANSYS mechanical. This research investigation helps in determining appropriate parameters with varied coated inserts to make the process easier, efficient and economical.

***Keywords**: Machinability, Hastelloy C-276, Taguchi L9 array, Chip formation, Coated and Uncoated inserts, Tool temperature, Surface roughness, Cutting forces, Fuzzy lozic, Tool wear.*

1. INTRODUCTION

In current day scenario, because of revolutionary advancements and breakthrough in metallurgy sector, the ever-growing demand for advancements and selection of tool materials for machining is at peak. With the introduction of super alloys, the need evolved into a necessity. A super alloy is an alloy which depicts various enhanced characteristics like high quality mechanical strength, corrosion and thermal creep resistance, high oxidation resistance, and superior surface stability. PVD coating plays a major role out of available technologies for enhancing the wear properties of a tool inserts. PVD coatings are preferred for sharp edges where compressive stresses are favourable. While dry machining of nickel-based alloy, Oxidation, BUE (Built Up Edge) formation, adhesion and diffusion are the dominant tool wear mechanisms that can be observed. In this study, Hastelloy C-276 is considered as a workpiece material machined by multiple tools with varying parameters of spindle speed, depth of cut and feed rate. The effect of above selected parameters on surface finish, the temperature achieved and tool wear are investigated. Surface roughness depends predominantly with the varied feed rate. In this paper, surface roughness and flank wear are considered mainly for evaluation of the performance for a tool. The coated tools provide better tool life, less wear and better surface finish compared to the uncoated ones. And due to high strength of nickel based super alloy, unique properties like flank wear, chipping, cracking were observed at cutting edge by machining through coated carbide tools. Premature facture and chipping were observed in uncoated carbide inserts whereas in coated carbide inserts progressive wear was observed. Taguchi design approach is one of the favourable methods for design of experimentation using an orthogonal array. In this research work, Taguchi L9 array design is adopted for carrying out the turning process with varied spindle speed, feed rate and depth of cut. The output results like flank wear, crater wear, nose wear, chip morphology, surface finish, MRR, feed force and tool temperature are analysed by S/N (Signal to Noise) ratios and ANOVA (Analysis of Variance). Surface plots of output results are given based on the Taguchi techniques.

The remaining work of this analysis is categorized into 6 sections. In the 2nd section of this paper, detailed literature reviews of published works are listed out. In the 3rd section, all the equipments, materials and software used in the experimental work are listed out. Experimental methodology, varied opted Taguchi optimization techniques, observations of the carried work, design and simulations results of the inserts are listed out in the section 4. In section 5, results and brief discussions on the obtained results are given. Finally, conclusions of the carried research work had been highlighted.

2. LITERATURE REVIEW

In the recent day phenomenon, manufacturing industries are concerned with new tool inserts with varied nano

Received: March 2020; Accepted: April 2020
Correspondence to: Dega Nagaraju, School of Mechanical Engineering (SMEC), Vellore Institute of Technology (VIT), Vellore, Tamil Nadu, India
E-mail: deganagarajulc@gmail.com
doi: 10.5937/fme2003651B

coatings and design technologies for enhancing the mechanical properties of the machining tool insert. Ashok Kumar Sahoo and Bidyadhar Sahoo [1] did a relative report on multi-layered coated (TiN/TiCN /Al2O3/TiN) carbide tool(1880HV) and uncoated carbide tool(1430 HV) on machining of high carbon high chromium AISI D2 steel (26HRC) in dry environment. It was found that TiN coated carbide tool life was higher than that of uncoated tool by 30 times and the surface roughness values were also better for TiN coated tool. A.I. Fernández-Abia et al [2] analysed the performance when difficult to machine material are turned by PVD advanced tool. The coatings used for the work were: AlTiSiN (nACo®), AlCrSiN (nACRo®), AlTiN and TiAlCrN for machining of austenitic stainless steel. Results stated that tools with AlTiN and AlTiSiN (nACo®) coatings have less tool flank wear. It also concluded that PVD coatings are oriented for sharp edges where high compressive stresses are positive.

A. Thakur et al [3] conducted the comparative analysis on tool wear and chip characteristics of multilayer uncoated and coated carbide tools when used to machine NIMONIC C263. The experimentation was carried out in dry environment with different cutting speed (51 and 84 m/min) keeping a constant feed and depth of cut of 0.2mm/rev and 1mm respectively. The experimental work utilised the CVD multilayer (Tin/TiCN/Al2O3 /ZrCN) coated carbide tool for investigation. It was observed that the coefficient of chip reduction decreased with increase in cutting speed and machining duration. During dry machining the tool wear was characterised by adhesion and diffusion. With increase in cutting speed and duration of machining, the flank wear is increased. A. Thakur and S. Gangopadadhyay [4] compared the machining of a nickel based super alloy Incoloy 825 with multilayer (TiN/ TiAlN) PVD coated carbide tool under dry machining and uncoated cemented carbide tool under wet conditions i.e. conventional flood cooling and minimum quantity lubrication. The evaluation is done on basis of machining performance of both rough and finished modes. It was observed that the cutting forces were remarkably reduced in coated tools under dry conditions as compared to the uncoated tool under wet condition.

C. Ezilarasan et al [5] work investigated the surface roughness on varying cutting parameters. Work used PVD coated carbide tool to machine NIMONIC C263. Work took the amalgamation of low, medium and high cutting parameters according to Taguchi L27 array for conducting experiments. Investigation revealed the cutting parameter which significantly influenced the surface roughness was feed rate. Chetan et al [6] studied the effect of the LN2 environment in the process of machining NIMONIC 90 using AlTiN coated and uncoated Tungsten carbide inserts. The paper explained the importance of the superalloy in aerospace industry and also enhancement of the properties in dry mode and compared the machining of the tool in dry mode and LN2 environment. It was found that the in LN2 environment the uncoated tool had less force than the coated tool in dry environment. The reduced in notch wear and edge fracture were observed in the LN2 environment. Also the chip fragments adhering over the rake face of uncoated tool was prevented in LN2 environment.

Yahya Işık [7] investigated different coatings on machining ability in the turning of steel. The tools selected for cutting for this research were PVD TiAlN coated, and CVD TiC + TiN, TiN coated carbide tool. The cutting forces along with wear were observed during the experimentation till the failure of the tool. It was observed the flank wear was most prominent in the experiment. With increase in cutting forces the flank wear increases. It was found that the flank wear of PVD coated TiALN was less that all other coatings which were used for the investigation. TiAlN coated tool provided 3 times tool life than the other coatings. K. Kadirgama et al [8] investigated the tool life of Hastalloy c-22HS when machined with carbide tool coated with PVD TiAlN, Tin/TiN; and CVD TiN/Al2O3, TiN cutting tool. It was studied that with increasing cutting speed axial depth the tool life decreases, feed rate is responsible parameter which affect the life of tool. Wear mechanism which were seen are Adhesion, Build-up-edge and oxidation. While machining Hastelloy Flank wear, catastrophic plastic lowering at cutting edge were observed.

Mohammad Akmal et al [9] studied the effects of AlTiN coatings by slot milling Ti6Al4V and compared it with end mills made up of uncoated solid carbide. The paper has utilized magnetic, friction finishing technique to evaluate the cutting forces and frictional coefficient. The article established a relation between frictional coefficient for the tool and workpiece pair. It was concluded that the coated tool gave less cutting forces than the uncoated one. M. Günay et al [10] investigated cutting tool stress in hard turning. The work has used the FEA by using ANSYS to study the stress. The cutting forces have been found at different machining parameters of cutting speed, feed rate and DOC. The work has utilised DIN 1.2344 tool steel (55+-1 HRC) as the workpiece material and uncoated ceramic insert as cutting tool. It was concluded from the study that then cutting forces changes with change of feed and depth of cut but had little change with change of cutting force. It was also found that the tool stress had inverse relation with cutting speed and direct relation with feed rate.

Nitin M. Mali and T. Mahender [11] did a comparative study of multilayer coated ceramic tool (Al2O3 +TiC+TiN+AlCrN) under dry machining with uncoated ceramic tool in CNC lathe for machining of hardened AISI 4340 steel (46 HRC). They used Taguchi L9 array for design of experiments. The work also used the digital microscope for the wear test. It was observed that the coated tool had less wear than the uncoated tool and the life of tool of the coated was higher while uncoated ceramic failed at 7th experiment. R Ravi Raja Malarvannam et al [12] investigated the effects of HSS single point cutting tool on coating it bilaterally with TiN and then followed by AlCrN using PVD technique. The work used scanning electron microscope to analyse the wear and microstructure, energy dispersive X-ray spectrum (EDX) to analyse composition and Optical microscope to analyse microstructure. It was seen that the coated HSS tool had 4.41 times higher tool life than uncoated tool. It was also found that the bilaterally coated HSS tool had better surface finish, higher surface hardness and higher wear resistance than the uncoated tool.

Leemet et al [13] investigated coating for a milling operation to check its suitability and quality. The work used commercial monolayer (Til-xAlx)N, nanocomposite (nc-Til-xAlxN)/(a-Si3N4) and (nc-Cel-xAlxN) /(a-Si3N4) coatings. Scanning electron microscope was used to determine wear. It concluded that flank wear width is observed as the key factor for tool life criteria. In practice several other indication of worn tool are used shape and colour of the chip, machined surface etc. Zhiqiang Liang et al [14] investigated the effects of coating on the cutting performance of micro endmills. A series of machining experiments were performed on Ti6Al4V with several materials. The end flank wear and the total cutting edge reduction were also studied. It was observed that there was a reduction of cutting edge chipping. It was also seen that coated tools gave more tool life and the surface finish of workpiece Ti6AL4V was better for coated tools. Abrasion and Adhesive wear on the tool flank face and rake face were determined as the dominant wear mechanism.

Davoodi and Eskandari [15] studied surface damages during turning of iron nickel base super alloy. Tamang and Chandrasekharan [16] performed experimental analysis on tool wear, surface roughness and temperature distribution. Das et al [17] studied effect of process parameters during machining of aluminium alloy by opting optimization techniques. Rajbongshi and Sharma [18] studied effect of parameters during machining of hardened steel by coated carbide tool in dry and as well as in force air cooling condition. Jahan et al [19] studied the significance of TiN, TiCN, AlTiN on WC inserts. Fountas et al [20] studied the optimum cutting parameters during machining of stainless steel flakes. Bongale and khedkar [21], studied wear of the tool while machining of low carbon steel. Lazarević et al [22], studied effect of nose radius, depth of cut, feed rate and cutting velocity on the cutting force. Tóth-Laufer and Horváth [23], stuied the effect of depth of cut, feed rate and cutting velocity on the surface integrity. Popović et al [24], investigated the chip morphology for considering the tool as 16MnCr5. Puzović and Kokotović [25], studied an approach which is used for modelling of turning cutting forces. Karabegović et al [26], studied the influence of depth of cut and cutting velocity on the tool acceleration and deformation.

Unlike all aforementioned research articles, this research paper addresses experimental analysis on the machinability of nicked based super alloy i.e. Hastelloy C-276. This hardened material has high strength, heat and corrosion resistance at high temperature. Therefore, in the present research work turning process was carried out on nickel based super alloy by using coated and uncoated inserts like coated HSS single point cutting insert, coated carbide inserts and uncoated ceramic insert. PVD coatings used on the inserts are HSN^2, Tinalox $SN^{2,}$ Alox SN^2, Hyperlox. Finally optimum parameters are obtained with respect to the calculated results like crater wear, flank wear, nose wear, MRR and surface roughness.

3. TAGUCHI OPTIMIZATION DESIGN

Taguchi optimization design is adopted to optimize the welding parameters. Generally, the technique involves, increase in the number of levels and time taken for experimental analysis. It also requires financial and time extensions to complete the multiple levels for experimental outputs. Hence, the research article is particularly carried out for orthogonal L9 as shown in the below table 1. It is a standard optimisation design that needs minimum numbers of level to identify the influence of welding parameters on final weldment. The required number of experiments to be done is given by the expression:

$$N_{Taguchi} = 1 + N_v\,(L\text{-}1)$$

$N_{Taguchi}$ = Number of experiments to be performed

N_v = Number of variables

L = number of Level

Dr. Taguchi introduced unique metrics, named as S/N ratios, to evaluate system's vigorousness. These metrics guide technicians for making decisions in optimizing process. The product performance may vary, which can be viable to various reasons. The reasons for the variability are named as noise factors. Noise factors may cause deviation of performance measures or functionality measures from its triggered value. Basically, an S/N ratio restrains the changes in a system due to noise factors. S/N ratio characteristics can be defined by various variables and choosing under this variety for optimal results is a challenging task. Preferably adopted features of S/N ratio in quality control engineering are:
Larger-the-better characteristics;

$$\text{S/N Ratio} = -10\log_{10}\left(1/n\right)\sum_{i=1}^{n}\frac{1}{y_{ij}^2} \tag{1}$$

Smaller-the-better characteristics;

$$\text{S/N Ratio} = -10\log_{10}\left(1/n\right)\sum_{i=1}^{n}y_{ij}^2 \tag{2}$$

Nominal-the-better characteristics;

$$\text{S/N Ratio} = -10\log_{10}\left(\frac{\bar{y}}{S_y^2}\right) \tag{3}$$

where y_i is the observed value through experimentation and n is the nuumber of trails of each experiment. $\bar{y}$ is the mean of experimentally observed data and S_y^2 is the variance of observed data. For each response, with S/N transformation, the larger the S/N ratio the betetr is the result.

Table 1: Taguchi orthogonal L9 array experimental design.

Experimental Runs	Process Parmeters		
	Land (mm)	Current (Amps)	Gas Flow Rate (Lit/min)
1	.5	100	12
2	.5	125	14
3	.5	150	16
4	1	100	14
5	1	125	16
6	1	150	12
7	1.5	100	16
8	1.5	125	12
9	1.5	150	14

Taguchi's method is used to get the optimal set of process parameters, for each output response individually by considering each production measure as unit response. The S/N ratio is employed to characterize quality response and the highest S/N is considered. Higher-the-better, and Lower-the-better process of S/N is applied for all output parameters respectively. As shown in the above table, 3 process parameters (land, current and gasflow rate) are considered.

4. METHODOLOGY

Machining of a superalloy is always a challenge and even a slight improvement can result in a significant profit. Hastelloy C-276 is one such superalloy and finding the most suitable tools with appropriate parameters and conditions will be very helpful for industrial purposes. This article focuses on optimising the significant machining parameters with combination of coated and uncoated tool inserts. Coated and uncoated carbide inserts, ceramic inserts and coated HSS tools were used for turning operation on Hastelloy C-276 cylindrical rod by varying speed of spindle, feed rate of lathe and depth of cut. The experimental procedure is carried out on NC machine. The temperature is measured to determine the need and type of lubrication during machining. For experiment purpose, the machining tools selected for machining of Hastelloy are, Tin Coated carbide insert, Tungsten carbide insert, CBN insert, Alumina- TiC based Ceramic insert

A cylindrical rod of Hastelloy C-276 with diameter 50 mm and 120 mm length is considered as work material. Commercially available Tin Coated carbide insert, Tungsten carbide insert, CBN insert and Alumina- TiC based Ceramic insert are utilized and their performance characteristics are compared. Surface roughness is estimated utilizing a roughness test at three different locations for each run and afterwards average value is measured. An instrument-work thermocouple is utilized to approximately estimate cutting temperature. Machining force was calculated analytically. Each type of wear of the cutting tools is determined using stereo zoom microscope after each experimental trail. The turning is done with three cause parameters viz. cutting speeds (Vc), i.e. 450, 710 and 1120 rpm. Three different feed (f) i.e. 0.05, 0.1, 0.16 mm/rev and depth of cut (ap) i.e. 0.2, 0.4, 0.6 mm were used to carry out the experiment. 20mm length was fixed for turning for each experimental run after which the tool is released for estimating wear of tool and surface roughness. At the end of the experimental run the values of all the parameters are calculated and noted for subsequent discussions.

Wear and surface roughness are also measured after each iteration. Finally, optimization is done using Mini tab software which is based on the Taguchi analysis method to achieve required objective. Physical, mechanical and chemical composition of the hardened steel i.e. Hastelloy C-276 is shown in the below tables 7 and 8. Initially, machining process is performed by using the coated single point cutting tool without any inserts. The geometry of the single point cutting tool and the selected tool insert are shown in the below table 2 and 4. And, mechanical properties of Tungsten carbide (WC) insert and CBN coated carbide insert are shown in the below tables 5 and 6. Finally, material, structure, colour and microhardness of the coatings used are listed in the below table 3.

Table 2: Geometry of the tool being used for the experiments

Front cutting edge angle	8°
End clearance angle	8°
Side rake angle	6°
Back rake angle	4°
Side clearance angle	6°

Table 3: Properties of the coatings used

Coating	Coating Material	Coating Structure	Colour	Microhardness [HV0.05]
HSN^2	2nd gen TiAlxN	Nanocomposite	Golden	3800
Tinalox SN^2	2nd gen TiAlN	Nanocomposite	Black Anthracite	3500
Hyperlox	2nd gen AlTiN	Nanocomposite	Black Anthracite	3700

Table 4: Geometry of the insert used

Circumcircle (d) in mm	Thickness (t) in mm	Radius (r) in mm
12.7	4.6	0.8

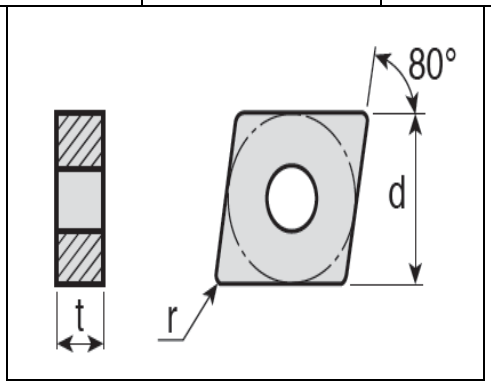

Table 5: Properties of CBN coated carbide tool

Indentation hardness (kg/mm2)	4,500
Compressive strength (GPa)	43-47
Modulus of elasticity (GPa)	600-800
Thermal conductivity (W/m-°K)	150-700

Table 6: Properties of WC insert

Properties	Minimum Value (S.I.)	Maximum Value (S.I.)	Units (S.I.)
Compressive Strength	3347	6833	MPa
Hardness	17000	36000	MPa
Modulus of rigidity	243	283	GPa
Tensile Strength	370	530	MPa
Modulus of elasticity	600	686	GPa
Thermal Conductivity	28	88	W/m.K

Table 7: Composition of Hastelloy C-276

Elements	Ni	Cr	Co	Mo	Mn	Fe	W	V	Si	C
Composition (%)	57	15.5	2.5	16	1	5.5	4	0.35	0.08	0.01

Table 8: Physical and Mechanical properties of Hastelloy C-276

Properties	Metric
Density	8.89 g/cm3
Melting Point	1371 °C
Tensile strength	601.2 MPa
Tensile strength	204.8 MPa
Elastic modulus	205 GPa
Rockwell Hardness	B 87
Thermal expansion co-efficient	11.2 µm/m°C
Thermal conductivity	11.2 µm/m°C

5. SIMULATION

Static structural analysis of the tool insert along with the tool holder was performed using ANSYS mechanical. The analysis was performed to check the area of vulnerability during machining and verify it with the tool wear images. For analysis, the tool and holder are first designed on SOLIDWORKS and then saved in the format of .STEP to be able to import the assembly in ANSYS can be seen in the below Figure 1. After importing the assembly, the geometric conditions, material for insert and tool holder were defined. All the important contact surface between tool insert and tool holder were defined. For meshing purpose, Global mesh was created and later uniform mesh of 3mm was generated and updated in the model. To get more accurate results at the insert, mesh refinement was performed for 1mm size. To create real life environment for simulation, the body of the tool holder was defined as fixed support. The forces were applied at the upper edge of the tool nose. Equivalent stresses, distortion and elastic strains generated near the nose radius of the tool insert are shown in the below Figures 2, 3 and 4. By the simulation results shown in below figures, technician can decide the actual life time of the inserts and can also analyse the selection of inserts with high quality matreial which can resist to the deformation and strains generated during machining without experimental runs.

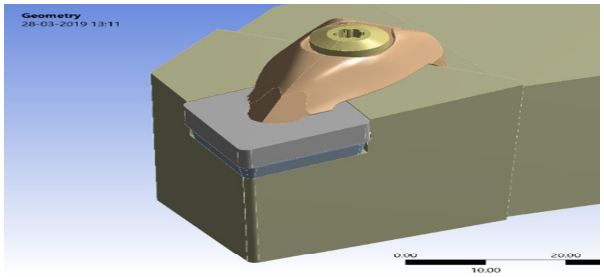

Figure 1. Design of tool holder and insert in Solidworks.

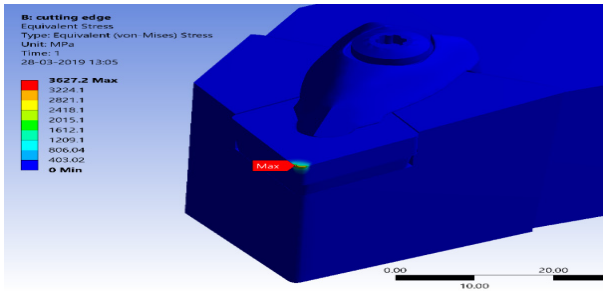

Figure 2. Equivalent stress on the tool insert

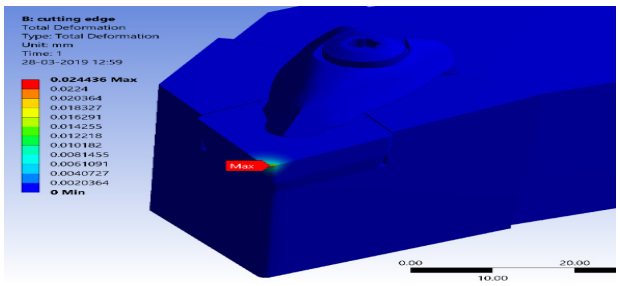

Figure 3. Total deformation of the tool insert

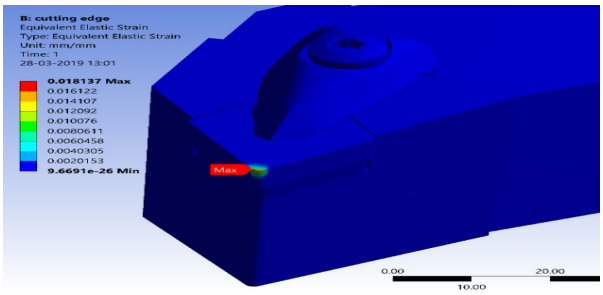

Figure 4. Equivalent elastic strain on the tool insert

6. RESULTS AND DISCUSSIONS

6.1 Observation of wear on coated single point cutting tool

The wear of the solid single point cutting tools are shown in below Figures 5 to 8 after few trials. Since the cutting edge was completely damaged, further experimentation couldn't be continued and hence we switched to inserts. Cutting edge could have been made again by grinding but it would have damaged the coating on HSS tools. From the figures highlighted below, it can be concluded that for machining of hardened materials, single point cutting tools either with coating or non-coating are not preferrable. Inserts are efficient tools for machining of hardened materials. Hence, same set of experimentaion is performed with 4 different inserts which is mentioned before.

Figure 5. HSN2 tool after 1st trial

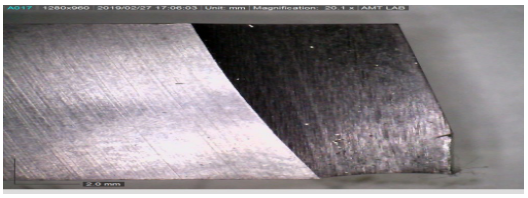

Figure 6. Hyperlox tool after 1st trial

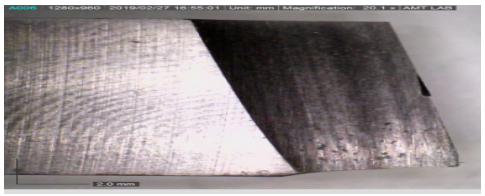

Figure 7. Tinalox tool after 1st trial

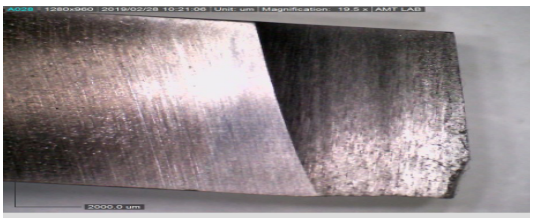

Figure 8. Alox tool after 3rd trial

6.2 Comparative analysis of different inserts based on varied parameters

Based on comparison of different inserts, one insert can be chosen for turning operation on Hastelloy C-276 for single objective optimization by Taguchi analysis. Major parameters used for comparison are Temperature, surface roughness, feed force and MRR.

Temperature

From Figure 9 shown below it is evident that after all the experimental trials least temperature was observed in ceramic inserts. Thus ceramic inserts are the best insert for machining of workpiece vulnerable to damage at high temperature.

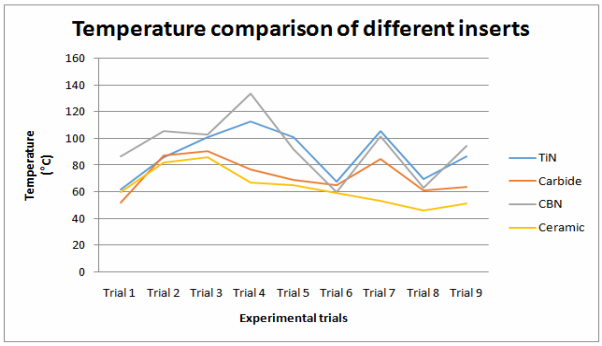

Figure 9. Temperature comparison of different insert

Surface Roughness

From the below Figure 10, CBN insert demonstrated the least surface roughness for almost all experiment trials and ceramic the most due to high wear rate.

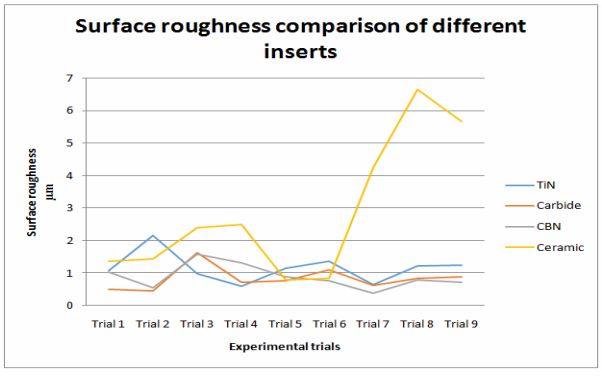

Figure 10. Surface roughness comparison of different inserts

Feed Force

The feed force followed a similar trend for almost all inserts at every experimental trial i.e. can be seen from the Figure 11. In CBN coated insert least forces were observed thus making it less prone to wearing and damaging.

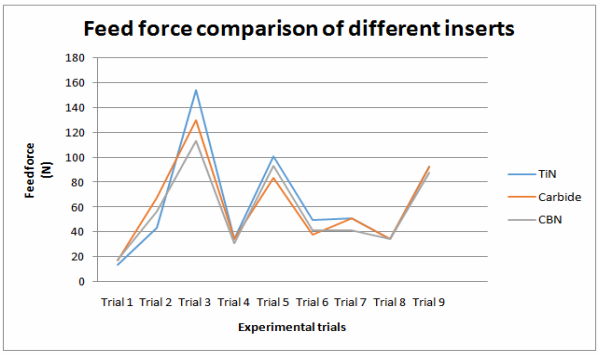

Figure 11. Feed force comparison of different inserts

Material Removal Rate

It is evident from the Figure 12 that CBN coated inserts have the highest MRR and thus can be an efficient option for machining of Hastelloy C-276.

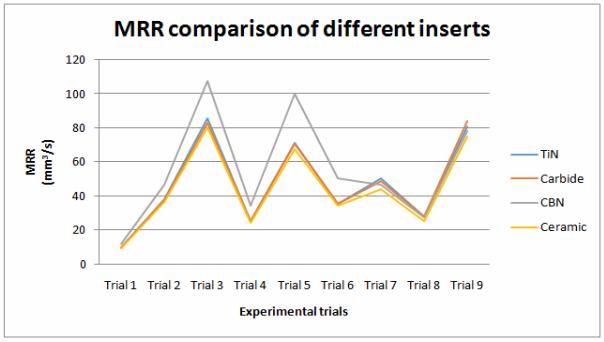

Figure 12. MRR comparison of different inserts

6.3 Single objective optimization of CBN coated insert using Taguchi analysis

After analysing the different parameters, it can be inferred that CBN coated Tungsten carbide insert performed better than other inserts and thus we choose it for single objective optimization using Taguchi analysis. Further analysis will help us in determining optimum parameters and will be our final result.

Effects of input parameters on tool temperature

Table 9: SN Ratio table for temperature with different input parameters

Level	A	B	C
1	-38.21	-39.14	-36.47
2	-39.27	-38.56	-39.51
3	-38.73	-38.51	-40.23
Delta	1.06	0.63	3.76
Rank	2	3	1

The tool temperature's average response value can be seen in Table. 9, it displays the rank of process parameters in order of speed of spindle, depth of cut and feed rate respectively. Response graph can be seen in Figure 13 and it can be inferred from the graph that the optimal combination of procedure parameters to achieve least tool temperature are speed of spindle at 1120RPM, feed at 0.16 mm/rev and cut depth of 0.2mm.

The surface plots help us to understand effects on combination of 2 parameters considered simultaneously. Figure 14 depicts following observations :

With increment in speed of spindle and decrease in depth of cut simultaneously, the tool temperature tends to reduce. With increment in feed rate and decrease in depth of cut simultaneously, the tool temperature tends to reduce.

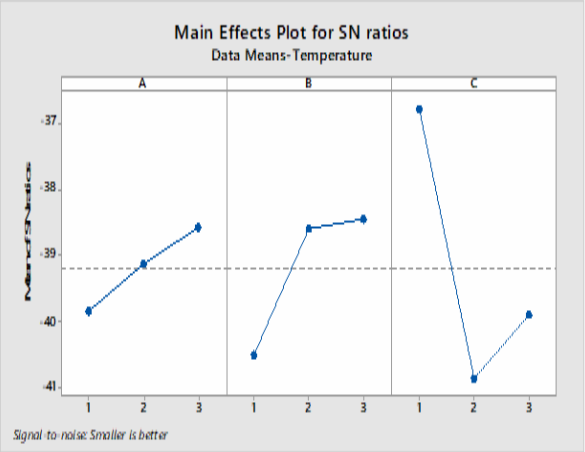

Figure 13. S/N ration graph for tool temperature with different input parameters

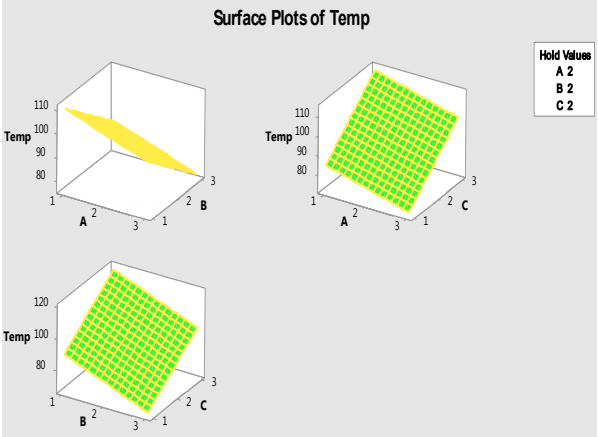

Figure 14. Surface plots of tool temperature with a combination of 2 parameters

Regression Equation; Temperature = 55.9 + 2.33 A - 4.17 B + 18.00 C

Table 10: ANOVA for temperature

	Degrees of Freedom	Adjusted Sum of Squares	Adjusted Mean Square	F-Value	P-Value
A	1	32.67	32.67	0.27	0.27
B	1	104.17	104.17	0.85	0.85
C	1	1944.00	1944.00	15.92	0.010
Error	5	610.72	122.14		
Total	8	2691.56			

Table 11: Predicted Values (for temperature)

Standard error	R-square	Adjusted R-square	Prediction R-square
11.0519	77.31%	63.70%	30.17%

Among various objectives of input parameters by analysing S/N ratio graphs and regression equation, depth of cut mostly depends on tool temperature. ANOVA is calculated to examine the percentage influence of procedure parameters on tool temperature during turning operation. ANOVA values are given in Table 10. This model is 77.31% fit and thus it can be used to predict temperature at any value of input parameters i.e. can be seen from the table 11.

Effects of input parameters on surface roughness

Table 12: SN Ratio table for surface roughness with different input parameters

1	-2.41338	2.40809	-1.73395
2	0.08630	-3.23398	-1.41582
3	-0.04523	-1.54642	0.77746
Delta	2.49968	5.64207	2.51141
Rank	3	1	2

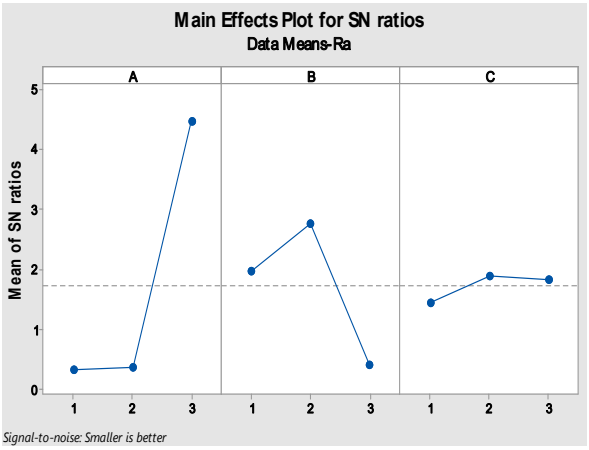

Figure 15. S/N ration graph for surface roughness with different input parameters

The surface roughness of the workpiece's average response value can be seen in Table. 12, it displays the rank of process parameters in order of Speed of spindle, Feed rate and Cut depth respectively. Response graph can be seen in Figure 15 and it can be inferred from the graph that the optimal combination of procedure parameters to achieve least surface roughness are Speed of spindle at 1120 RPM, feed at 0.1 mm/rev and Cut depth 0.4mm.

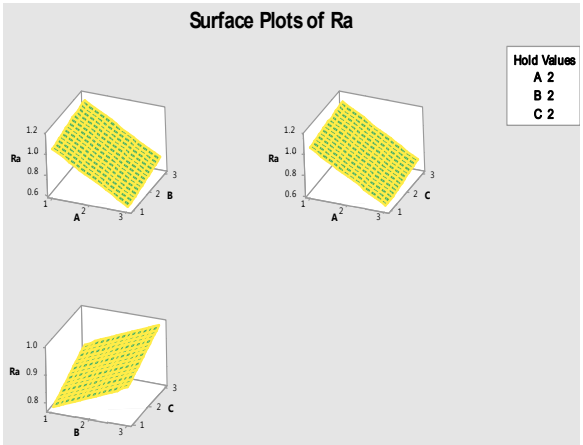

Figure 16. Surface plots of surface roughness with a combination of 2 parameters

The surface plots help us to understand effects on combination of 2 parameters considered simultaneously. Figure 16 depicts following observations :

With increment in speed of spindle and decrement in feed rate simultaneously, the surface roughness will be

reduced. With increment in speed of spindle and decrease in depth of cut simultaneously, the surface roughness tends to reduce. With decrease in feed rate and decrease in depth of cut simultaneously, the surface roughness tends to reduce.

Regression Equation; Ra = 1.396 - 0.181 A + 0.211 B - 0.145 C

Table 13: ANOVA for surface roughness

	Degrees of Freedom	Adjusted Sum of Squares	Adjusted Mean Square	F-Value	P-Value
A	1	0.1973	0.1973	0.94	0.376
B	1	0.2684	0.2684	1.28	0.308
C	1	0.1253	0.1253	0.60	0.474
Error	5	1.0447	0.2089		
Total	8	1.6357			

Among various objectives of input parametrs by analysing S/N ratio graphs and regression equation, feed rate mostly depends on surface roughness. ANOVA is calculated to measure the percentage influence of procedure parameters on surface roughness in the process of turning operation. ANOVA values are given in Table 13.

Effects of input parameters on feed force

Table 14: SN Ratio table for feed force with different input parameters

Level	A	B	C
1	-33.22	-29.34	-29.25
2	-34.96	-34.59	-34.34
3	-34.80	-39.04	-39.38
Delta	1.74	1.74	10.13
Rank	3	2	1

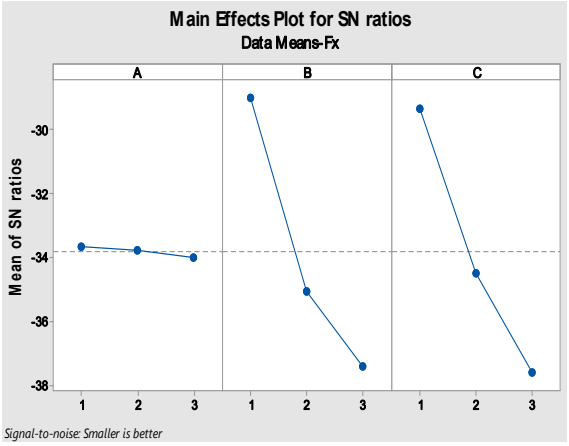

Figure 17. S/N ration graph for feed force with different input parameters

The feed force's average response value can be seen in Table. 14, it displays the rank of process parameters among speed of spindle, feed rate and Cut depth. Response graph can be seen in Figure 17 and it can be inferred from the graph that the optimal combination of procedure parameters to achieve least feed force are Speed of spindle at 450 RPM, Feed rate at 0.05 mm/rev and depth of cut 0.2mm.

The surface plots help us to understand effects on combination of 2 parameters considered simultaneously. Figure 18 depicts following observations :

With increment in speed of spindle and decrement in feed rate simultaneously, the feed force tends to reduce. With increment in speed of spindle and decrease in depth of cut simultaneously, the feed force tends to reduce. With decrease in feed rate and decrease in depth of cut simultaneously, the feed force tends to reduce.

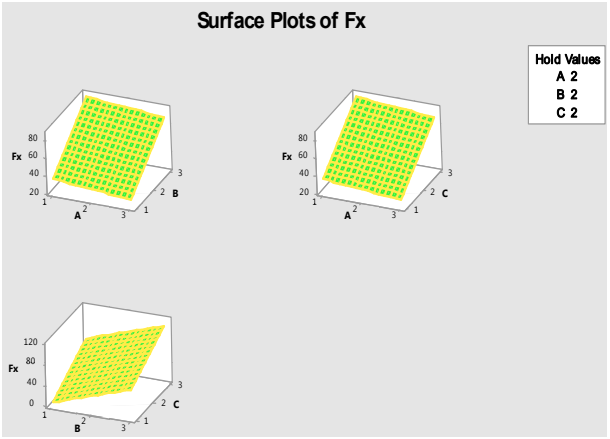

Figure 18. Surface plots of feed force with a combination of 2 parameters

Regression Equation; Fx = -60.0 - 5.59 A + 32.88 B + 34.82 C

Table 14: ANOVA for feed force

	Degrees of Freedom	Adjusted Sum of Squares	Adjusted Mean Square	F-Value	P-Value
A	1	187.4	187.4	0.64	0.462
B	1	6485.3	6485.3	22.00	0.005
C	1	7273.4	7273.4	24.67	0.004
Error	5	1474.2	294.8		
Total	8	15420.3			

Table 15: Predicted values (for feed force)

Standard error	R-square	Adjusted R-square	Prediction R-square
17. 171%	90.44%	84.7%	63.56%

Among various objectives of input parametrs by analysing S/N ratio graphs and regression equation, depth of cut mostly depends on feed force. ANOVA is calculated to measure the percentage influence of procedure parameters on tool temperature during turning operation. ANOVA values are given in Table 14 . This model is 90.44% fit and thus it can be used to predict feed force at any value of input paramteres i.e can be seen from the table 15.

Effects of input parameters on crater wear

Table 16: SN Ratio table for crater wear with different input parameters

Level	A	B	C
1	-113.3	-111.2	-116.9
2	-112.5	-116.1	-111.4
3	-119.2	-117.7	-116.7
Delta	6.7	6.4	5.4
Rank	1	2	3

The crater wear of tool's average response value can be seen in Table. 16, it displays the rank of process

parameters among speed of spindle, feed rate and depth of cut. Response graph can be in Figure 19 and it can be inferred from the graph that the optimal combination of procedure parameters to achieve least crater wear are Speed of spindle at 450 RPM, Feed at 0.05 mm/rev and Cut depth of 0.4 mm.

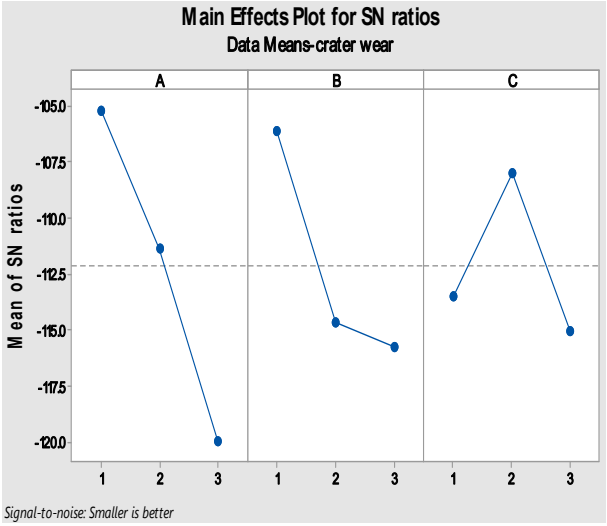

Figure 19. S/N ration graph for crater wear with different input parameters

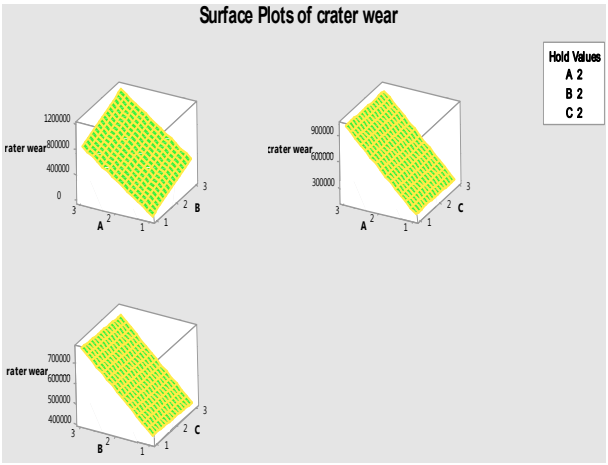

Figure 20. Surface plots of crater wear with a combination of 2 parameters

Table 17: ANOVA for crater wear

	Degrees of freedom	Adjusted sum of squares	Adjusted Mean Square	F-Value	P-Value
A	1	3.06169E+11	3.06169E+11	8.17	0.035
B	1	1.47902E+11	1.47902E+11	3.95	0.104
C	1	1727926128	1727926128	0.05	0.838
Error	5	1.87390E+11	37477983113		
Total	8	6.43189E+11			

The surface plots help us to understand effects on combination of 2 parameters considered simultaneously. Figure 20 depicts following observations :

With decrement in speed of spindle and decrease in feed rate simultaneously, the crater wear tends to reduce. With decrease in speed of spindle at particular depth of cut, the crater wear tends to reduce. With decrease in feed rate and increase in depth of cut simultaneously, the crater wear tends to reduce.

Regression Equation; Crater Wear = -86869 + 225894 A + 157004 B - 16970 C

Table 18: Predicted values (for crater wear)

Standard error	R-square	Adjusted R-square	Prediction R-square
193592	70.87%	53.38%	6.94%

Among various objectives of input parameters by examining S/N ratio graphs and regression equation, speed of spindle has maximum influence on crater wear. ANOVA is calculated to measure the percentage influence of procedure parameters on crater wearduring turning operation. ANOVA values are given in Table 17 . This model is 70.87% fit and thus it can be used to predict crater wearat any value of input parameters i.e. can be seen from the table 18.

Effects of input parameters on flank wear

Table 19: SN Ratio table for flank wear with different input parameters

Level	A	B	C
1	-112.5	-123.1	-124.6
2	-125.5	-117.7	-117.0
3	-128.8	-126.0	-125.2
Delta	16.3	8.3	8.2
Rank	1	2	3

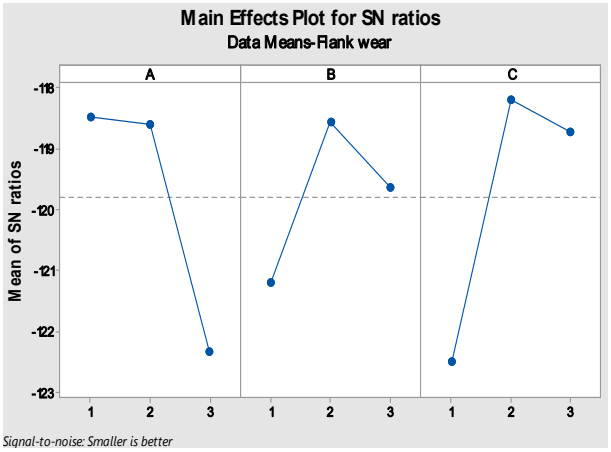

Figure 21. S/N ration graph for flank wear with different input parameters

The flank wear's average response value can be seen in Table. 19, it displays the rank of process parameters among speed of spindle, feed rate and depth of cut. Response graph can be seen in Figure 21 and it can be inferred from the graph that the optimal combination of procedure parameters to achieve least flank wear are Speed of spindle at 450 RPM, Feed rate at 0.1 mm/rev and depth of cut 0.4 mm.

The surface plots help us to understand effects on combination of 2 parameters considered simultaneously. Figure 22 depicts following observations :

With increment in speed of spindle and decrement in feed rate simultaneously, the feed force tends to reduce. With increment in speed of spindle and decrease in depth of cut simultaneously, the feed force tends to

reduce. With decrease in feed rate and decrease in depth of cut simultaneously, the feed force tends to reduce.

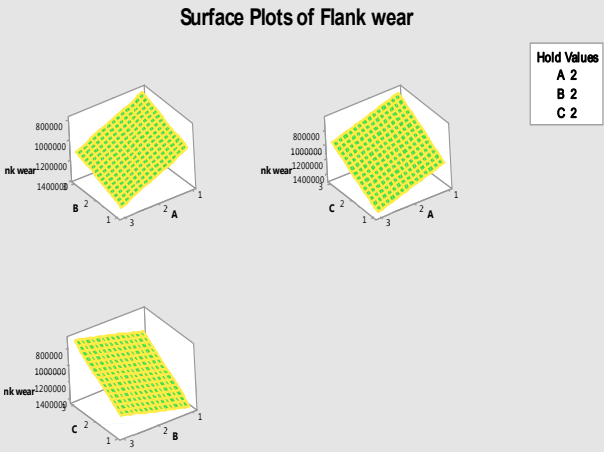

Figure 22. Surface plots of flank wear with a combination of 2 parameters

Regression Equation; Flank Wear = -881815 + 1040951 A + 292115 B + 4145 C

Table 20: ANOVA for flank wear

	Degrees of freedom	Adjusted sum of squares	Adjusted Mean Square	F-Value	P-Value
A	1	6.50147E+12	6.50147E+12	42.66	0.001
B	1	5.11986E+11	5.11986E+11	3.36	0.126
C	1	103066255	103066255	0.00	0.980
Error	5	7.62005E+11	1.52401E+11		
Total	8	7.77556E+12			

Table 21: Predicted values (for flank wear)

Standard error	R-square	Adjusted R-square	Prediction R-square
390386	90.20%	84.32%	71.46%

Among various objectives of input parameters by examining S/N ratio graphs and regression equation, speed of spindle has maximum influence on flank wear. ANOVA is calculated to measure the percentage influence of procedure parameters on flank wearduring turning operation. ANOVA values are given in Table 20 . This model is 90.20% fit and thus it can be used to predict flank wearat any value of input parameters i.e. can be seen from the table 21.

Effects of input parameters on nose wear

Table 22: SN Ratio table for nose wear with different input parameters

Level	A	B	C
1	-118.1	-119.9	-119.7
2	-123.1	-121.4	-121.9
3	-123.8	-123.7	-123.4
Delta	5.7	3.8	3.7
Rank	1	2	3

The nose wear of the tool's average response value can be seen in Table. 22, it displays the rank of process parameters in order of speed of spindle, feed rate and depth of cut respectively. Response graph can be seen in Figure 23 and it can be inferred from the graph that the optimal combination of procedure parameters to achieve least nose wear are speed of spindle at 450 RPM, Feed at 0.1 mm/rev and Cut depth of 0.2 mm.

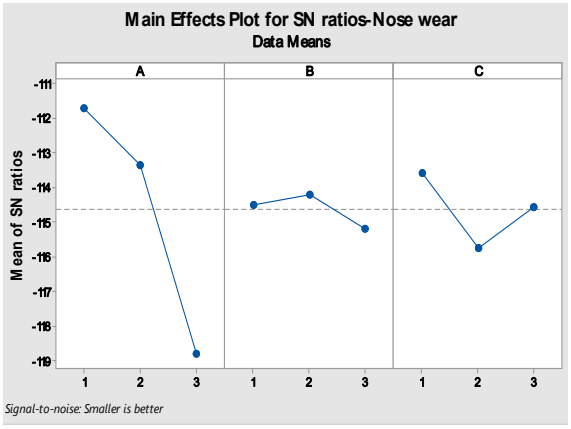

Figure 23. SN ratio graph for nose wear with different input parameters

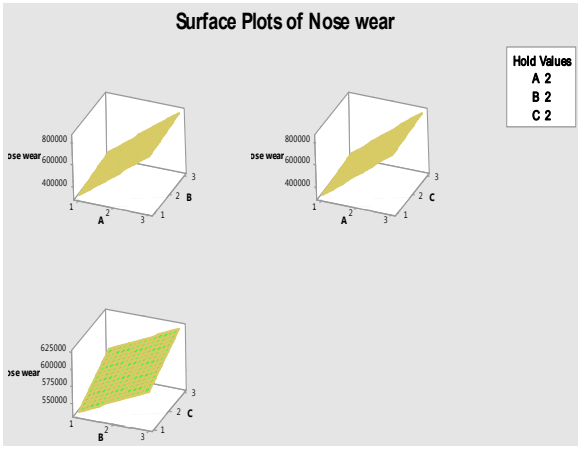

Figure 24. Surface plots of nose wear with a combination of 2 parameters

The surface plots help us to understand effects on combination of 2 parameters considered simultaneously. Figure 24 depicts following observations :

With decrement in speed of spindle and decrease in feed rate simultaneously, the nose wear tends to reduce. With decrease in speed of spindle and decrement in depth of cut at a time, the nose wear tends to decrease. With decrement in feed rate and decrease in depth of cut simultaneously, the nose radius tends to reduce.

Regression Equation; Nose Wear = -85730 + 310440 A + 194462 B + 188494 C

Table 23: ANOVA for nose wear

	Degrees of freedom	Adjusted sum of squares	Adjusted Mean Square	F-Value	P-Value
A	1	5.78237E+11	5.78237E+11	7.64	0.040
B	1	2.26892E+11	2.26892E+11	3.00	0.144
C	1	2.13179E+11	2.13179E+11	2.82	0.154
Error	5	3.78448E+11	75689547382		
Total	8	1.39676E+12			

Table 24: Predicted values (for nose wear)

Standard error	R-square	Adjusted R-square	Prediction R-square
275117	72.91%	56.65%	12.21%

Among various objectives of input parametrs by analysing S/N ratio graphs and regression equation, speed of spindle has maximum influence on nose wear. Analysis of variance is calculated to measure the percentage influence of process parameters on nose wear during turning operation. ANOVA values are given in Table 23. This model is 72.91% fit and thus it can be used to predict nose wear at any value of input parameteres i.e. can be seen from the table 24.

Effects of input parameters on MRR

Table 25: SN Ratio table for MRR with different input parameters

Level	A	B	C
1	30.04	27.35	26.62
2	32.09	32.55	32.64
3	33.75	35.97	36.61
Delta	3.71	8.61	10.00
Rank	3	2	1

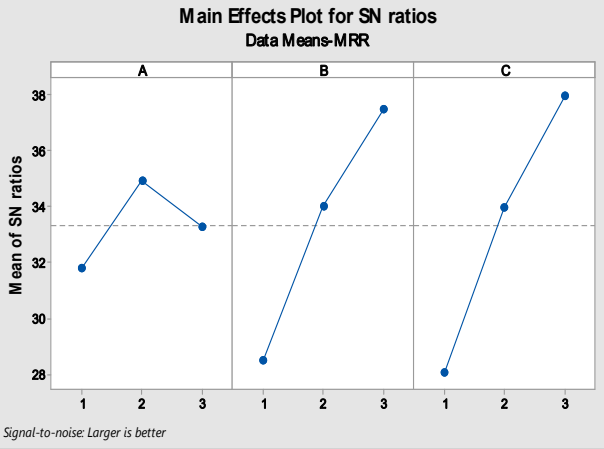

Figure 25. S/N ratio graph for MRR with different input parameters

The Material removal rate (MRR) of the workpiece's average response value can be seen in Table. 25, it displays the rank of process parameters among speed of spindle, feed rate and depth of cut respectively. Response graph is shown in Figure 25 and it can be inferred from the graph that the optimal combination of procedure parameters to achieve least nose wear are speed of spindle at 710 RPM, feed at 0.16 mm/rev and Cut depth 0.6mm.

The surface plots help us to understand effects on combination of 2 parameters considered simultaneously. Figure 26 depicts following observations :

With decrement in speed of spindle and increase in feed rate simultaneously, the MRR tends to increase. With decrease in speed of spindle and increment in depth of cut simultaneously, the MRR tends to increase. With increment in feed rate and increment in depth of cut simultaneously, the MRR tends to increase.

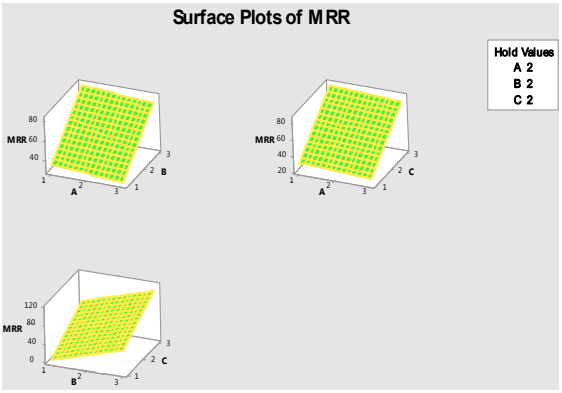

Figure 26. Surface plots of MRR with a combination of 2 parameters

Regression Equation; MRR = -45.0 + 4.34 A + 19.43 B + 22.38 C

Table 26: ANNOVA for Material Removal Rate

Source	Degrees of freedom	Adjusted sum of squares	Adjusted Mean Square	F-Value	P-Value
A	1	113.0	113.01	1.89	0.228
B	1	2266.1	2266.14	37.83	0.002
C	1	3005.7	3005.70	50.18	0.001
Error	5	299.5	59.90		
Total	8	5684.3			

Table 27: Predicted values (for MRR)

Standard error	R-square	Adjusted R-square	Prediction R-square
7.73947	94.73%	91.57%	78.28%

Among various objectives of input parametrs by analysing S/N ratio graphs and regression equation, depth of cut has maximcum influence on MRR. ANOVA is calculated to determine the percentage influence of procedure parameters on MRR in the process of turning operation. ANOVA values are given in Table 26. This model is 94.73% fit and thus it can be used to predict feed force at any value of input parameters i.e. can be seen from the table 26.

Table 28: Observation of TiN coated carbide insert

RPM	Feed (mm/rev)	Depth of cut (mm)	Temp (°C)	Ra (µm)	Crater Wear µm^2	Flank Wear µm^2	Nose Wear µm^2
450	0.05	0.2	62	1.075	442613.5	825331.4	429498.5
450	0.1	0.4	86	2.156	407100.6	79135.42	760149.6
450	0.16	0.6	101	0.993	540452.8	1144255	1590894
710	0.05	0.4	113	0.608	629197.4	1432362	1528698
710	0.1	0.6	101	1.156	702047.4	2135586	1385355
710	0.16	0.2	68	1.381	837937.4	2222347	1371768
1120	0.05	0.6	106	0.666	848772.2	2481117	1478952
1120	0.1	0.2	70	1.226	912542.7	2688412	1522973
1120	0.16	0.4	87	1.244	984217.3	3124896	1641256

Table 29: Observation of Tungsten carbide insert

RPM	Feed (mm/rev)	Depth of cut (mm)	Temp (°C)	Ra (µm)	Crater Wear µm^2	Flank Wear µm^2	Nose Wear µm^2
450	0.05	0.2	52	0.489	101448.2	221402.7	148997.2
450	0.1	0.4	88	0.451	228319.5	536512.1	422657.2
450	0.16	0.6	91	1.628	3119045	1398604	995065.6
710	0.05	0.4	77	0.713	3168009	2201609	1736479
710	0.1	0.6	69	0.756	3273404	3576256	2007952
710	0.16	0.2	65	1.088	4541358	1883778	2009706
1120	0.05	0.6	85	0.609	4974841	201225.3	2414522
1120	0.1	0.2	61	0.836	5112412	382256.8	2536987
1120	0.16	0.4	64	0.889	5854136	447715.2	2988734

Table 30: Observation of CBN insert

RPM	Feed (mm/rev)	Depth of cut (mm)	Temp (°C)	Ra (µm)	Crater Wear µm^2	Flank Wear µm^2	Nose Wear µm^2
450	0.05	0.2	87	1.019	114875.2	1885209	312677.2
450	0.1	0.4	106	0.558	211132.6	492383.5	391285.8
450	0.16	0.6	103	1.572	244900.5	637558.1	468918.9
710	0.05	0.4	134	1.3	72907.03	726942.3	599693.9
710	0.1	0.6	92	0.884	748700.8	916262.9	408305.3
710	0.16	0.2	60	0.769	916290.1	926511.5	412013.8
1120	0.05	0.6	102	0.382	979006.9	1104455.7	799741.5
1120	0.1	0.2	63	0.778	994571.5	1352154.5	845712.8
1120	0.16	0.4	95	0.718	1021133.2	1497752.5	981112.1

Table 31: Observation of Alumina- TiC based Ceramic insert

RPM	Feed (mm/rev)	Depth of cut (mm)	Temp (°C)	Ra (µm)	Crater Wear µm^2	Flank Wear µm^2	Nose Wear µm^2
450	0.05	0.2	60	1.373	59366.571	1141226.28	1031049.21
450	0.1	0.4	82	1.452	778253.941	2543317.95	2403451.97
450	0.16	0.6	86	2.412	836857.124	4539486.84	5768984.99
710	0.05	0.4	67	2.507	1056974.662	5591316.96	6664197.23
710	0.1	0.6	65	0.793	1282417.9	6986379.3	854358.123
710	0.16	0.2	36	0.842	1385481.8	8911178.9	9725463.12
1120	0.05	0.6	53	4.259	1496663.32	10124567.2	11755698.3
1120	0.1	0.2	46	6.647	1635487.236	11978645.8	12854618.3
1120	0.16	0.4	51	5.662	1801238.754	13016477.3	14574284.5

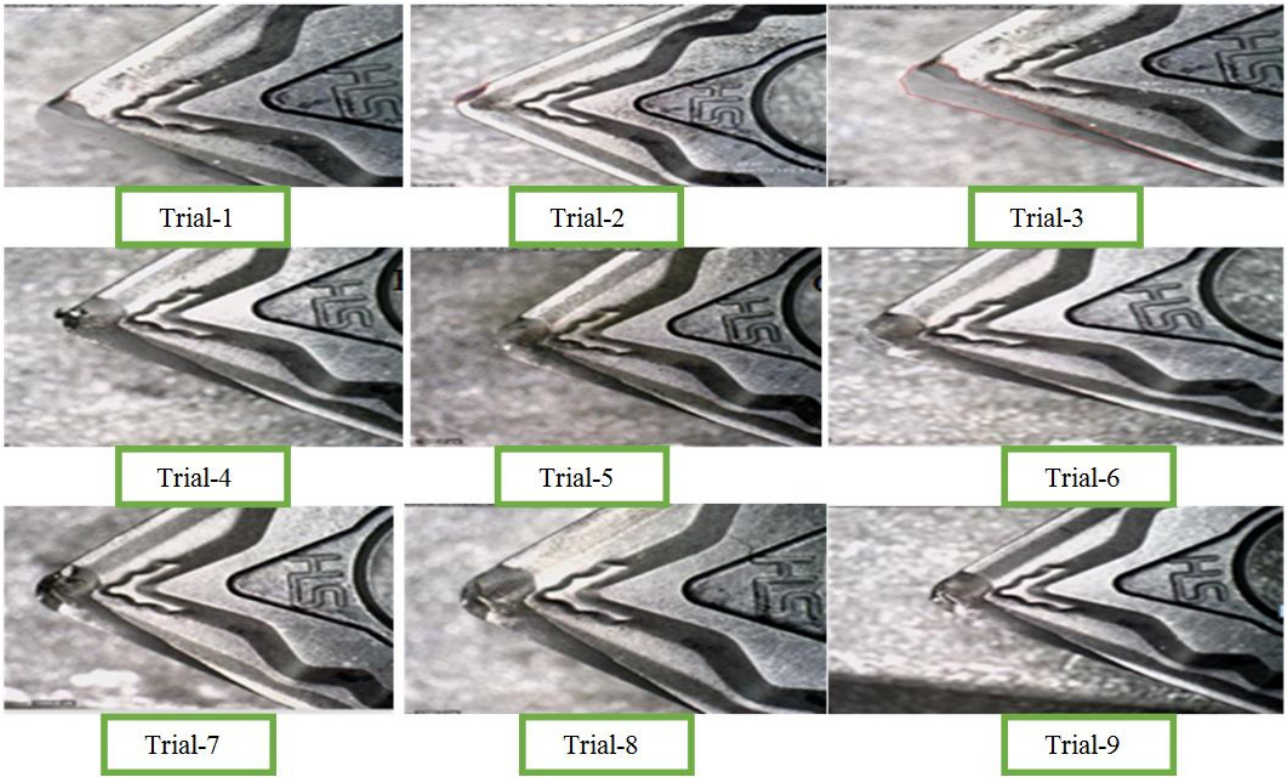

Figure 27. Crater wear of W-Carbide tool after each trial.

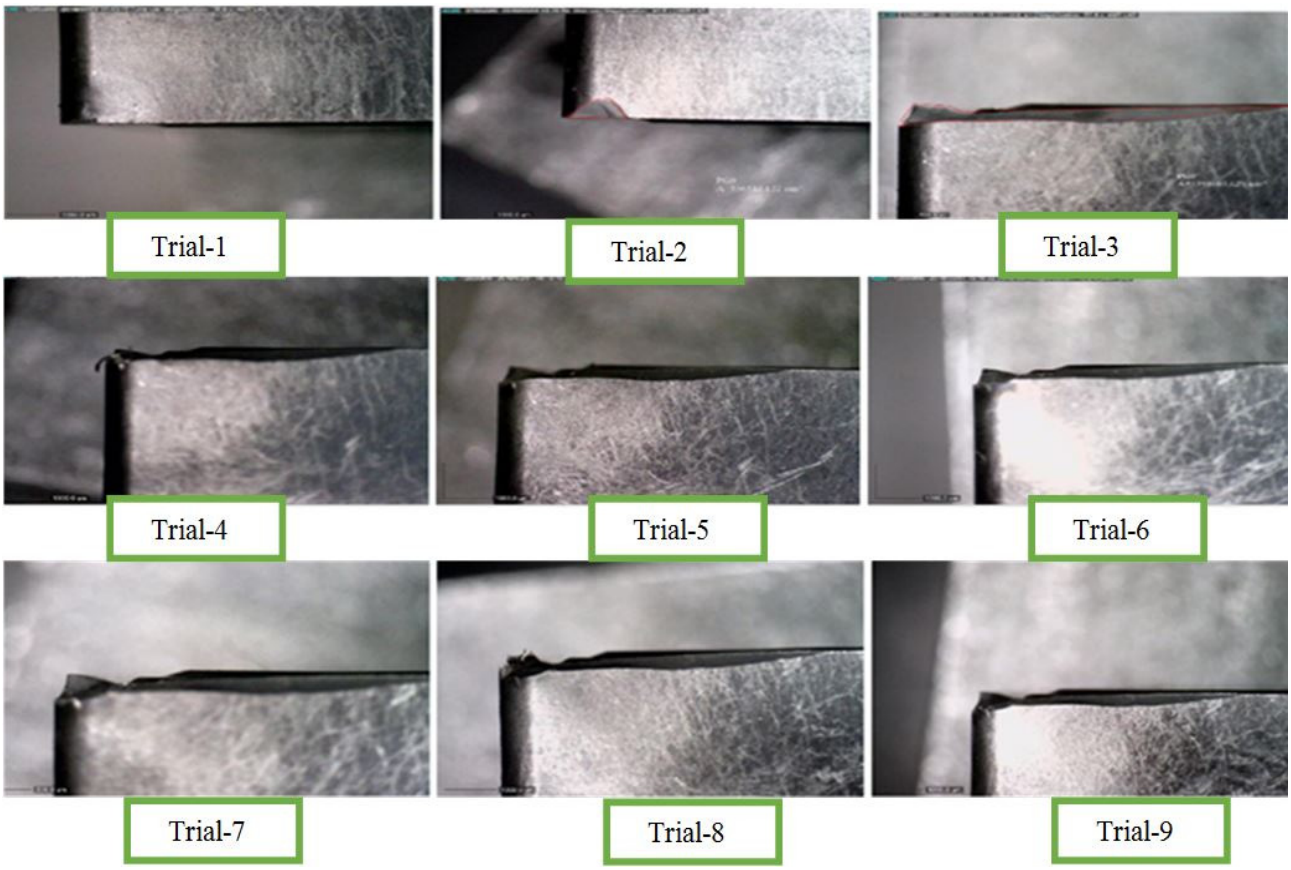

Figure 28. Flank wear of W-Carbide tool after each trial.

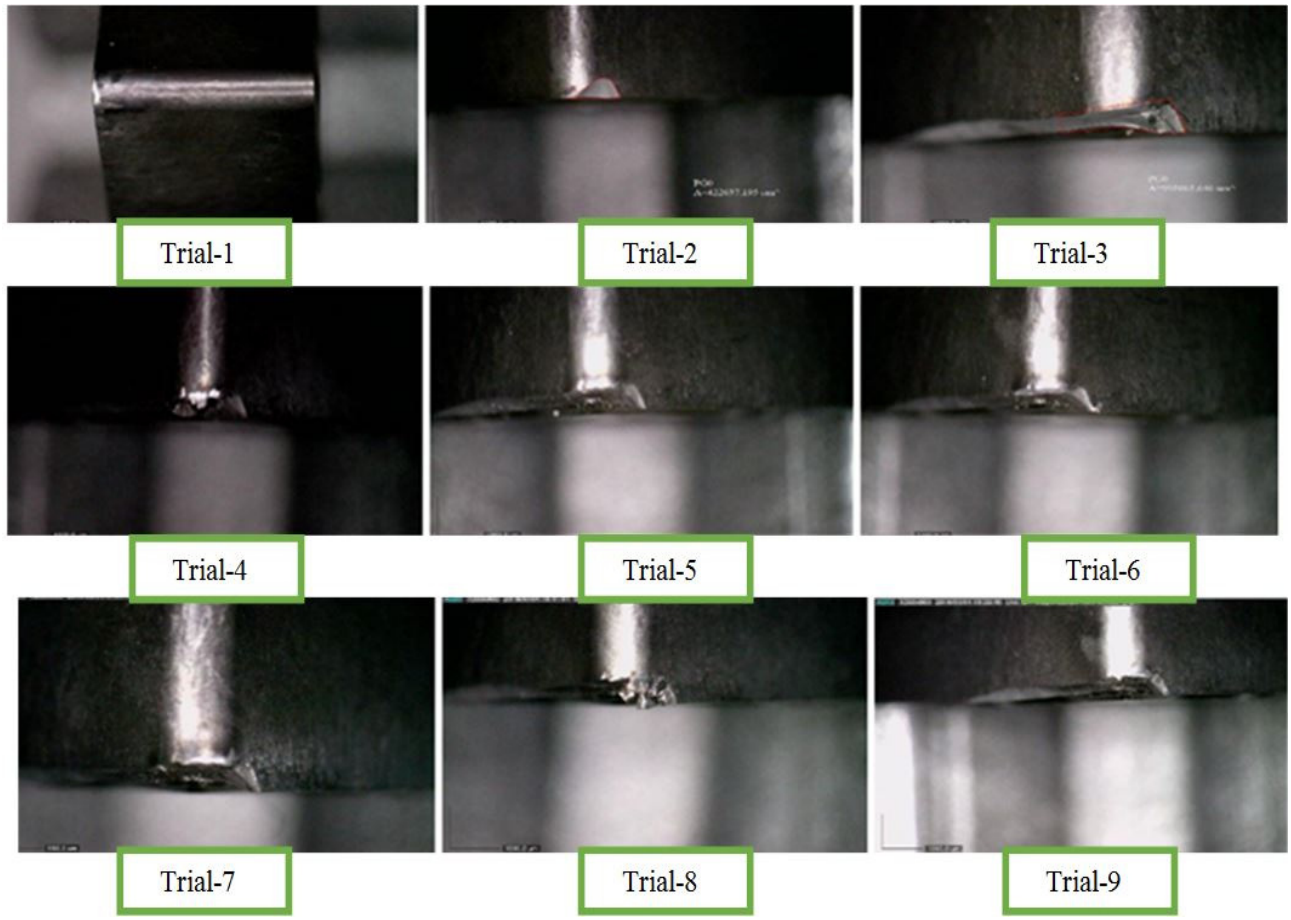

Figure 29. Nose wear of W-Carbide tool after each trial.

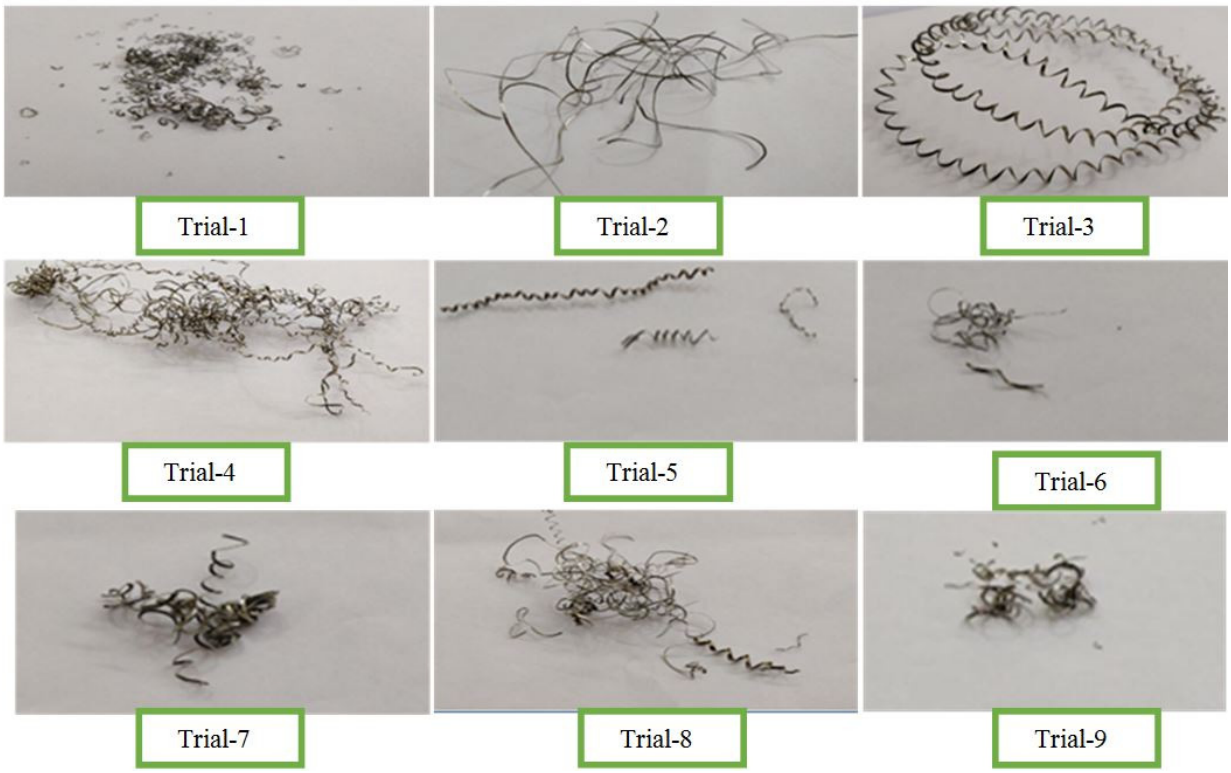

Figure 30. Chip morphology of Tin coated carbide tool after each trial.

6.4 Observation of wears on inserts

The same set of experimentation was then done on 4 types of inserts already mentioned before. The observation table for the 4 inserts are given in below tables 28 to 31.

Crater Wear

Crater wear occurs in the contact region of tool face and chip. Maximum amount of generated heat is carried away by the chip. Hence, when the chips come in contact with the rake face of the tool it generates crater wear. Frequently, BUE formation can also be observed on the rake face of the tool during dry machining. It can be seen from Figure 27.

Flank Wear

Flank wear occurs in the contact region of tool and workpiece. Frequently, flank wear formation can be observed on the flank face of the tool due to high friction and micro chips. It can be seen from Figure 28.

Nose Wear

Flank wear occurs at the nose of tool. Nose wear formation can be observed on the nose of the tool due to abrasive wear. This wear results in increase in increasing of rake angle which leads to decrease the effectiveness of the tool. It can be seen from Figure 29.

Chip Morphology

Formation of continuous, discontinuous and serrated chips are observed at varied spindle speed, depth of cut and feed rate. It can be seen from Figure 30.

7. CONCLUSIONS

This paper aimed at optimizing the machining characteristics of Hastelloy C-276 Super alloy with the help of single objective optimization using Taguchi design of experiments methodology. There are two sections in conclusion as the analysis was completed in two parts.

Conclusions from comparative analysis

For Hastelloy C-276, machining can be done by using ceramic inserts since least temperature was observed in all the experimental trials. For smoothing process, CBN coated tungsten carbide insert can be used for machining Hastelloy C-276 since it gave the least surface roughness. To achieve prolonged tool life, CBN coated tungsten carbide can be used as it faces least feed force during machining. For efficient machining, CBN coated carbide tool can be used as it gives maximum MRR.

Above points conclude that CBN coated carbide inserts is most suitable for machining Hastelloy C-276 and thus is further analysed using Taguchi analysis for optimization of parameters.

Conclusions from Single objective optimization using Taguchi analysis:

In order to improve Tool Temperature response characteristics using Taguchi analysis, depth of cut must be adjusted as it has the highest impact on it. There is an least impact of Rate of feed on the process. The optimal combination of procedure parameters to achieve least tool temperature are spindle speed at 1120 RPM, feed rate at 0.16 mm/rev and depth of cut 0.2mm. In order to improve surface roughness response characteristics using Taguchi analysis, feed rate must be adjusted as it has the highest impact on it. Spindle speed has the least impact on the process. The optimal combination of procedure parameters to achieve least surface roughness are spindle speed at 1120 RPM, feed rate at 0.1 mm/rev and depth of cut 0.4mm. In order to improve feed force (Fx) response characteristics using Taguchi analysis,

depth of cut must be adjusted as it has the highest impact on it. Spindle speed has the least impact on the process. The optimal combination of procedure parameters to achieve least feed force are spindle speed at 450 RPM, feed rate at 0.05 mm/rev and depth of cut 0.2mm. In order to improve crater wear response characteristics using Taguchi analysis, spindle speed must be adjusted as it has the highest impact on it. Depth of cut has the least impact on the process. The optimal combination of process parameters to achieve least crater wear are Spindle speed at 450 RPM, Feed rate at 0.05 mm/rev and depth of cut 0.4 mm. In order to improve flank wear response characteristics using Taguchi analysis, spindle speed must be adjusted as it has the highest impact on it. Depth of cut has the least impact on the process. The optimal combination of process parameters to achieve least flank wear are Speed of spindle at 450 RPM, Rate of feed at 0.1 mm/rev and Cut depth 0.4 mm. In order to improve nose wear response characteristics using Taguchi analysis, spindle speed must be adjusted as it has the highest impact on it. Depth of cut has the least impact on the process. The optimal combination of process parameters to achieve least nose wear are Speed of spindle at 450 RPM, Rate of feed at 0.1 mm/rev and Cut depth 0.2 mm. In order to improve MRR response characteristics using Taguchi analysis, depth of cut must be adjusted as it has the highest impact on it. Spindle speed has the least impact on the process. The optimal combination of process parameters to achieve least nose wear are spindle speed at 710 RPM, feed rate at 0.16 mm/rev and depth of cut 0.6mm.

Moreover in further research works, the results of this turning process can be improved with some computational steps and it will be applicable in all the companies for modifying and solving the multi-objective problems.

REFERENCES

[1] Sahoo, Ashok Kumar, and Bidyadhar Sahoo. "Experimental investigations on machinability aspects in finish hard turning of AISI 4340 steel using uncoated and multilayer coated carbide inserts." *Measurement* 45, no. 8 (2012): pp. 2153-2165.

[2] Fernández-Abia, A. I., J. Barreiro, J. Fernández-Larrinoa, LN López de Lacalle, A. Fernández-Valdivielso, and O. M. Pereira. "Behaviour of PVD coatings in the turning of austenitic stainless steels." *Procedia Engineering* 63 (2013): pp. 133-141.

[3] Thakur, A., S. Gangopadhyay, A. Mohanty, and K. P. Maity. "Performance Evaluation Of CVD Multilayer Coating On Tool Wear Characteristics During Dry Machining Of Nimonic C-263." In *5th International & 26th All India Manufacturing Technology, Design And Research Conference (AIMTDR 2014) December 12th–14th*. 2014.

[4] Thakur, A., and S. Gangopadhyay. "Dry machining of nickel-based super alloy as a sustainable alternative using TiN/TiAlN coated tool." *Journal of cleaner production* 129 (2016): 256-268.

[5] Ezilarasan, C., VS Senthil Kumar, A. Velayudham, and K. Palanikumar. "Surface roughness analysis on machining of nimonic C–263 alloy using ANN and RSM techniques." *International Journal of Precision Technology* 2, no. 4 (2011): 340-354.

[6] Chetan*, A.Habtamu, B.C.Behera, S.Ghosh, P.V.Rao (2017) "Machining of Nimonic 90 Alloy Under Dry and LN2 Environment Using AlTiN Coated and Uncoated Tungsten Carbide Inserts" *proceeding of 10th Interntional conference on precision, Meso, Micro and Nano Engineering(COPEN 10)*

[7] Isik, Yahya. "Tool life and performance comparison of coated tools in metal cutting." *International Journal of Materials and Product Technology* 39, no. 3-4 (2010): 240-250.

[8] Kadirgama, K., K. A. Abou-El-Hossein, M. M. Noor, K. V. Sharma, and B. Mohammad. "Tool life and wear mechanism when machining Hastelloy C-22HS." *Wear* 270, no. 3-4 (2011): 258-268.

[9] Akmal, Mohammad, KS Ehsan Layegh, Ismail Lazoglu, Ali Akgün, and Çağlar Yavaş. "Friction coefficients on surface finish of AlTiN coated tools in the milling of Ti6Al4V." *Procedia CIRP* 58 (2017): 596-600.

[10] Günay, Mustafa, Mehmet Erdi Korkmaz, and Nafiz Yaşar. "Finite element modeling of tool stresses on ceramic tools in hard turning." *Mechanics* 23, no. 3 (2017): 432-440.

[11]Mali, Nitin M., and T. Mahender. "Wear Analysis Wear Analysis Of Single Point Cutting Tool Single Point Cutting Tool Single Point Cutting Tool With And With And With And Without Coating."

[12]Malarvannan, R., T. V. Moorthy, P. Hariharan, and P. Prabhu. "Investigation on HSS single point cutting tool manufactured using physical vapor deposition coating process." (2016).

[13]Leemet, T., J. Allas, and E. Adoberg. "TOOL WEAR INVESTIGATIONS BY DIRECT AND INDIRECT METHODS IN END MILLING."

[14]Liang, Zhiqiang, Peng Gao, Xibin Wang, Shidi Li, Tianfeng Zhou, and Junfeng Xiang. "Cutting performance of different coated micro end mills in machining of Ti-6Al-4V." *Micromachines* 9, no. 11 (2018): 568.

[15]Davoodi, Behnam, and Behzad Eskandari. "Evaluation of surface damage mechanisms and optimisation of cutting parameters in turning of N-155 iron-nickel-base superalloy." *International Journal of Machining and Machinability of Materials* 21, no. 1-2 (2019): 100-114.

[16]Tamang, S. K., M. Chandrasekaran, K. Palanikumar, and Ramanathan M. Arunachalam. "Machining performance optimisation of MQL-assisted turning of Inconel-825 superalloy using GA for industrial applications." *International Journal of Machining and Machinability of Materials* 21, no. 1-2 (2019): 43-65.

[17] Das, Diptikanta, Vivek Chakraborty, Bijaya Bijeta Nayak, Mantra Prasad Satpathy, and Chandrika

Samal. "Machining of aluminium-based metal matrix composite-a particle swarm optimisation approach." *International Journal of Machining and Machinability of Materials* 22, no. 1 (2020): 79-97.

[18] Rajbongshi, Sanjib K., and Deba Kumar Sarma. "A comparative study in prediction of surface roughness and flank wear using artificial neural network and response surface methodology method during hard turning in dry and forced air-cooling condition." *International Journal of Machining and Machinability of Materials* 21, no. 5-6 (2019): 390-436.

[19]Jahan, Muhammad P., Gregory K. Arbuckle, and Ann M. Rumsey. "A comparative study on the effectiveness of TiN, TiCN, and AlTiN coated carbide tools for dry micro-milling of aluminium, copper and brass at low spindle speed." *International Journal of Machining and Machinability of Materials* 20, no. 2 (2018): 141-164.

[20]Fountas, Nikolaos A., Georgios V. Seretis, Dimitrios E. Manolakos, Christopher G. Provatidis, and Nikolaos M. Vaxevanidis. "Multi-objective statistical analysis and optimisation in turning of aluminium matrix particulate composite using genetic algorithms." *International Journal of Machining and Machinability of Materials* 20, no. 3 (2018): 236-251.

[21]Bongale, Arunkumar, and Nitin Khedkar. "Machining Performance Evaluation of Liquid Nitrogen Treated M2 Cutting Tools for Turning Operations."

[22]Lazarević, D., Janković P., Madić M., Lazarević, A. "Robust conditions for cutting force minimization in polyamide turning process." *FME Transactions* 43, no. 2 (2015): 114-118.

[23]Tóth-Laufer, Edit, and Richárd Horváth. "Fuzzy model based surface roughness prediction of fine turning." *FME Transactions* 45, no. 1 (2017): 181-188.

[24]Popović, Mihajlo, Ljubodrag Tanović, and Kornel F. Ehmann. "Cutting forces prediction: The experimental identification of orthogonal cutting coefficients." *FME Transactions* 45, no. 4 (2017): 459-467.

[25]Puzović, Radovan, and Branko Kokotović. "Prediction of thrust force and torque in tapping operations using computer simulation." *FME Transactions* 34, no. 1 (2006): 1-5.

[26]Karabegović, Isak, Bekir Novkinić, and Ermin Husak. "Experimental identification of tool holder acceleration in the process of longitudinal turning." *FME Transactions* 43, no. 2 (2015): 131-137.

УПОРЕДНА АНАЛИЗА ПРОЦЕСНИХ ПАРАМЕТАРА КОД ХАБАЊА УМЕТАКА ЗА АЛАТ СА И БЕЗ ПРЕМАЗА ПРИ ОБРАДИ ЛЕГУРЕ HASTELLOY C-276

Б. Киран, Д. Нагарају

У сваком производном предузећу машинска обрада је најважнија у процесу побољшања квалитета готовог производа. У раду се анализира обрада легуре Hastelloy C-276 помоћу квалитетних PVD керамичких уметака за алат са премазом, без премаза и на бази алуминијума. Поступак стругања је вршен на NC машини варирањем RPM, брзине помоћног кретања и дубине резања према плану експеримента Тагучи L9. Истраживање је обухватило хабање коленастог вратила, хабање бочне стране, хабање врха, површинску храпавост, температуру алата и силу помака при обради чврстог материјала, а истовремено је извршена и статичка структурна анализа уметка за алат и држача алата помоћу ANSYS софтвера. Истраживање је од помоћи у одређивању одговарајућих параметара код различитих уметака са премазом да би се процес олакшао, био ефикаснији и економичнији.